energies

MDPI

Article

The Efficiency Prediction of the Laser Charging Based on GA-BP

Chengmin Wang [1,2], Guangji Li [1], Imran Ali [1,3], Hongchao Zhang [1], Han Tian [2] and Jian Lu [1,*]

[1] School of Science, Nanjing University of Science and Technology, Nanjing 210094, China; rosswang@jsei.edu.cn (C.W.); ligj@njust.edu.cn (G.L.); imran_phy142@yahoo.com (I.A.); hongchao@njust.edu.cn (H.Z.)
[2] School of Digital Equipment, Jiangsu Vocational College of Electronics and Information, Huai'an 223003, China; huaishi_tianhan@sina.com
[3] Department of Physics, University of Agriculture, Faisalabad 38040, Pakistan
* Correspondence: lj6805@njust.edu.cn

Abstract: In IoT applications, energy supply, especially wireless power transfer (WPT), has attracted the most attention in the relevant literature. In this paper, we present a new approach to laser irradiance solar cell panels and predicting energy transfer efficiency. From the previous experimental datasets, it has been discovered that in the laser charging (LC) process, temperature has a great impact on the efficiency, which is highly correlated with the laser intensity. Then, based on artificial neural network (ANN), we set the above temperature and laser intensity as inputs, and the efficiency as output through back propagation (BP) algorithm, and use neural network and BP to train and modify the network parameters to approach the real efficiency value. We also propose the genetic algorithm (GA) to optimize the learning rate of the BP, which achieved slightly superior results. The results of the experiment indicate that the prediction method reaches a high accuracy of about 99.4%. The research results in this paper provide an improved solution for the LC application, particularly the energy supply of IoT devices or small electronic devices through WPT.

Keywords: wireless power transfer; laser charging; BP; GA

Citation: Wang, C.; Li, G.; Ali, I.; Zhang, H.; Tian, H.; Lu, J. The Efficiency Prediction of the Laser Charging Based on GA-BP. *Energies* **2022**, *15*, 3143. https://doi.org/10.3390/en15093143

Academic Editors: Mauro Feliziani and Vítor Monteiro

Received: 26 March 2022
Accepted: 24 April 2022
Published: 25 April 2022

1. Introduction

Small electronic devices have an enormous application in modern society, such as IoT occasions. Their energy transfer essential character is wireless. Wireless power transfer (WPT) provides the convenient and essential energy transfer method of the IoT devices, and the most common form is electromagnetic (EM) induction [1]. Now, a brand-new laser charging (LC) method is presented that avoids the complex antenna adjusting and offers more long distance, easy settling, and more power transferring. LC presents a solar cell panel that is irradiated by the laser beam to harvest the photovoltaic power. Its diagram is shown as below [2]:

The outside continuous laser device emits the laser beam which is located on the 2-DOF platform. When the solar cells are irradiated by the laser, the photovoltaic power generates in the panel cells. The IoT application area classifies the energy management into two main models: 1. efficient solutions, and 2. harvesting operations [3]. Most reported dedicated methods of IoT energy systems are RF sources; nevertheless, LC is more suitable for a long-distance energy transfer and it high-energy density. In summary, LC provides an autonomous, long-distance, wireless, and constant power supply to the IoT nodes in smart city scenarios [4]. As the new method in WPT, few studies have discussed this. In summary, the theory of the LC and basic experiment devices was built [5,6]. The LaserMotive company made a UAV power charged by laser beam in a NASA report [7], while the limitation of LC implementation is the efficiency of the energy transform. Furthermore, how much laser power is needed to feed the application demand in advance? The answer is given in this paper, through construction of the Efficiency Prediction Model based on those experiment datasets.

2. Band Gap and Material of the Solar Cell

The main disadvantage of LC is the low efficiency of the energy transferring. Taking the new multiple-junction terrestrial cell used in this issue, named $In_{0.3}Ga_{0.7}As$, as a sample, its efficiency is about 37.9 ± 1.2% (under the global AM1.5 spectrum 1000 W/m^2 at 25 °C) [8,9]. From the literature [10] we obtain the ideal efficiency decided by the band gap under the fixed irradiated spectrum, which is called theoretical limit of efficiency.

$$\eta = \frac{E_g \int_{E_g}^{\infty} b_s(E, T_s) dE}{\int_0^{\infty} E b_s(E, T_s) dE} \quad (1)$$

The E_g is the band gap, and the integral items represent the energy of the spectral photon flux. It seems that the maximum conversion efficiency is raised by the band gap. However, the bigger band gap would cause difficulty of the electronic transition and a corresponding efficiency reduction. For any spectrum, there is an optimum band gap to achieve the highest efficiency.

Considering the laser irradiation circumstance, its spectrum is much narrower than the solar, so the LC's efficiency presents a better performance.

When the temperature is at 300 K, the ratio of element with the band gap of the solid solution varies, as per Formula (2):

$$E_g(x) = 0.354 + 0.604x + 0.475x^2 (\text{eV}) \quad (2)$$

The x is the ratio of the element **In**. Then x = 0.3, the band gap energy of $\mathbf{In_{0.3}Ga_{0.7}As}$ is 1.01 eV, which is the optimal band gap for photoelectric conversion with a wavelength around 1000 nm, such as 1070 nm. The atmospheric window is near 1000 nm while the corresponding bandgap is about 1.0 eV, and the latter is smaller than that in the solar irradiation, according to the previous experiments' data which are provided by the supplier: Shanghai Institute of Space Power-Sources [11]. Compared with the other materials, $In_{0.3}Ga_{0.7}As$ presents better conversion efficiency near the 1070 nm band [12,13] and the consequent conversion efficiency is about 35% under the lab testing environment.

3. Efficiency Variation under the Laser Intensity and Temperature

In the LC process, temperature, affecting the efficiency significantly, has high correlation with the laser intensity. As the laser energy increases, the temperature of the solar panel also increases, while the photovoltaic conversion efficiency linearly decreases sharply. Those potential relationships could be used to forecast the efficiency of the LC influenced by the intensity of the laser intensity and the corresponding temperature.

Through the experiment of Figure 1, we obtained a series of data concerned with laser density, temperature, and the efficiency during the PV process. The previous research mentioned that a strong correlation exists among laser density, temperature, and efficiency. Meanwhile, those correlations might be complicated and hard to draw theoretical conclusion from. Those correlations could be seen in Figures 2 and 3.

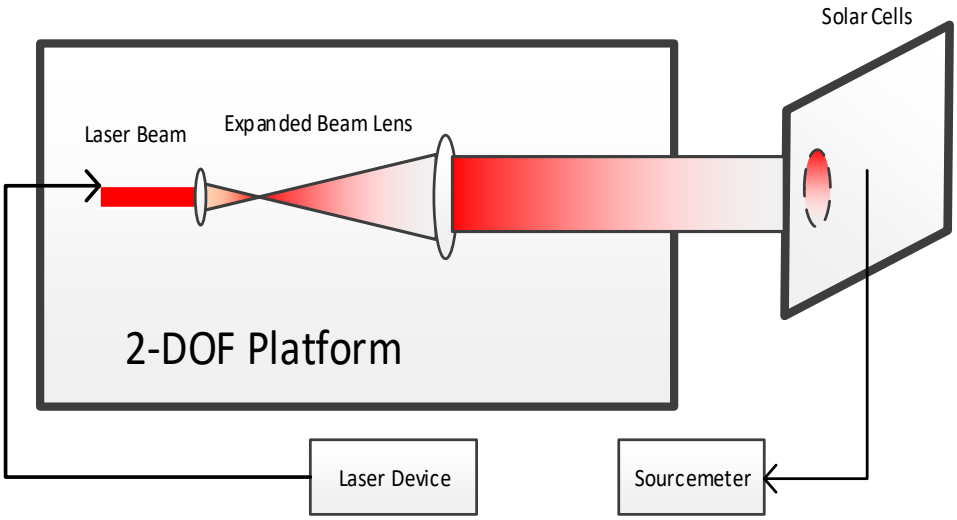

Figure 1. Schematic diagram of LC.

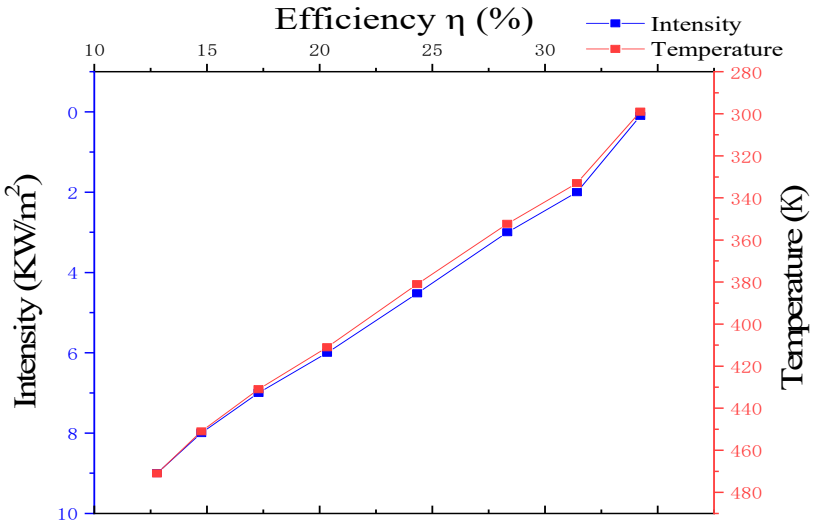

Figure 2. Efficiency curve under the different laser intensity and temperature.

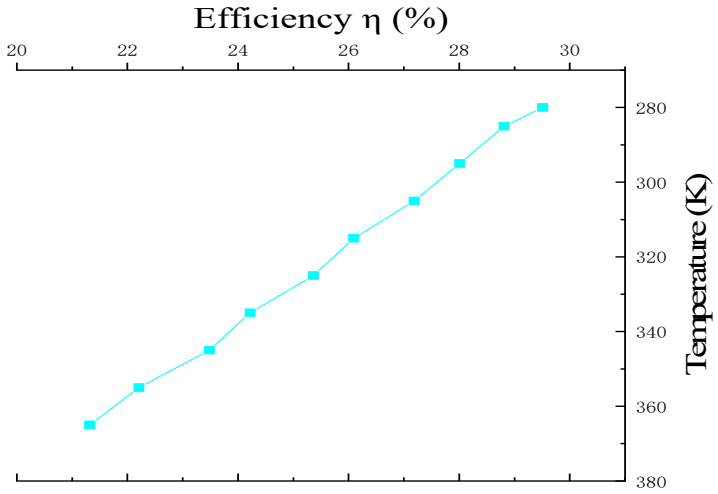

Figure 3. Efficiency curve under the fixed laser intensity (1 kw/m^2).

4. ANN (Artificial Neural Network) and Multi-Layer Perceptron (MLP)

4.1. ANN Components

Then, those experimental data could be built into models based on empirical nature. The idea of the solution method is the utilization of an artificial neural network (ANN). The main target of an ANN is to mimic information processing and knowledge acquisition in the human brain by developing mathematical algorithms. The ANN is the most magnificent active advance and has been prominent among researchers since 1980. ANNs have been used in an assortment of utilization, including displaying, classification, design acknowledgment, and multivariate information examination. ANN is widely used to predict the PV power generation efficiency in most research because of nonlinearity in meteorological data. ANN is a more appropriately contrasted and factual technique when a non-straight and complicated issue exists between the information with next to no earlier presumption [14].

In Figure 4, $x_1, x_2, x_3, \cdots x_n$ illustrate the various signals of intensity, and $w_1, w_2, w_3, \cdots w_n$ mean synaptic strength. Their sum of products, called ξ, compares the value of ξ with the threshold (also called bias, b) and could determine the output (y) of the neuron.

$$y = \begin{cases} 1, & if\ \xi \geq b \\ 0, & else \end{cases} \tag{3}$$

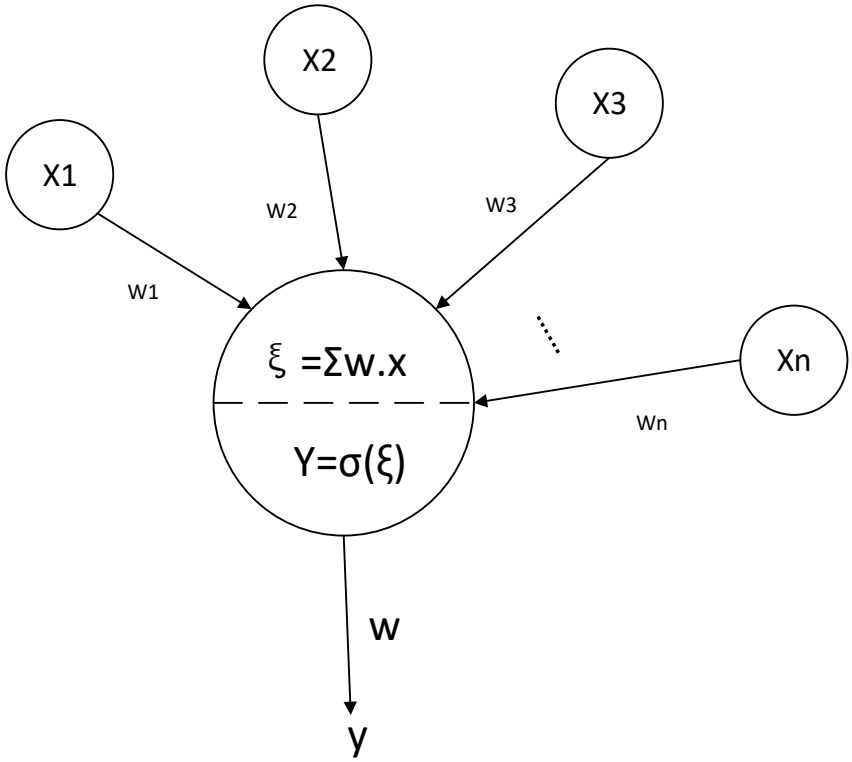

Figure 4. M (McCullough)–P (Pitts) neuron model.

Then, at that point, an activation function is applied to that result to diminish the plentifulness scope of the result signal y into a limited worth; various kinds of initiation capacities are available. Commonly, we use sigmoid function as:

$$f(\varphi) = \frac{1}{1+e^{-\varphi}}, \varphi = \sum w_i \cdot x_i \tag{4}$$

4.2. Back Propagation (BP) Algorithm

The single-layer perceptron could be trained under the setting rules which were designed first. The w and the threshold were modified to decide the error between the output y and the real one with the sample data. Nevertheless, single-layer perceptron just has one layer of functional neurons, which limits its learning ability. In order to meet the nonlinearly complicated problems, additional layer(s) of neurons placed between the input layer (containing input nodes) and the output neuron are needed, resulting in the multi-layer perceptron (MLP) architecture that includes input, output, and some hidden layers, as shown in Figure 5.

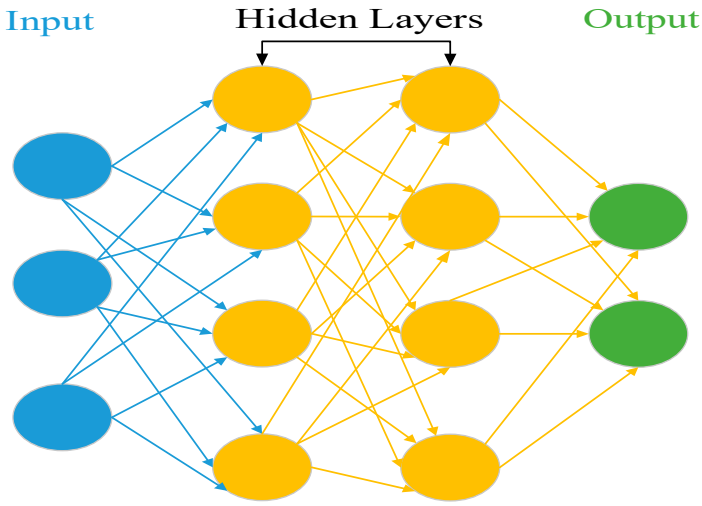

Figure 5. Typical MLP architecture.

Each layer's neurons are fully connected with the next layer's neurons, without connection between the same layer or cross layer in the common MLP architecture. This is the multi-layer feedforward neural network, which can be well trained by adjusting the connection weight w_i and the threshold b to make its learning function complete. This kind of training does not just utilize simple studying rules; it uses strong and powerful algorithms which use back propagation (BP) algorithms. BP performs better due to its prominence, adaptability, and flexibility in displaying a wide range of issues in numerous application regions.

BP searches an error surface (which serves as a function of ANN weights) using gradient descent based on the point(s) with the minimum error. The algorithm data flow is shown in Figure 6. Each BP iteration constitutes two scans: a forward activation that produces a solution and a backward propagation of the computational error that corrects the weights [15].

Forward processing:

$$In_{h_1} = x_1 \times w_{11} + x_2 \times w_{21}, \quad h_1 = Out_{h_1} = Sigmoid(In_{h_1}) \tag{5a}$$

$$In_{h_2} = x_1 \times w_{12} + x_2 \times w_{22}, \quad h_2 = Out_{h_2} = Sigmoid(In_{h_2}) \tag{5b}$$

$$In_o = h_1 \times w_{h_1} + h_2 \times w_{h_2} + \cdots + h_n \times w_{h_n}, \quad O = Out_o = sigmoid(In_o) \tag{5c}$$

$$Error = \frac{1}{2}(O - y)^2 \tag{5d}$$

y is the expected result.

Back propagation:

Based on the gradient descent strategy, the weights were changed by the negative direction of the output goals.

$$\delta_{h_1} = \frac{\partial Error}{\partial w_{h_1}} = \frac{\partial Error}{\partial O} \times \frac{\partial O}{\partial In_o} \times \frac{\partial In_o}{\partial w_{h_1}} \tag{6a}$$

where

$$\frac{\partial Error}{\partial O} = O - y, \quad \frac{\partial O}{\partial In_o} = O(1-O), \quad \frac{\partial In_o}{\partial w_{h_1}} = h_1 \tag{6b}$$

Likewise,

$$\delta_{h_2} = \frac{\partial Error}{\partial w_{22}} = \frac{\partial Error}{\partial O} \times \frac{\partial O}{\partial In_o} \times \frac{\partial In_o}{\partial w_{h_2}} \tag{6c}$$

$$\cdots \cdots$$

$$\delta_{11} = \frac{\partial Error}{\partial w_{11}} = \frac{\partial Error}{\partial O} \times \frac{\partial O}{\partial In_o} \times \frac{\partial In_o}{\partial h_1} \times \frac{\partial h_1}{\partial w_{11}} \tag{6d}$$

$$\delta_{12} = \frac{\partial Error}{\partial w_{12}} = \frac{\partial Error}{\partial O} \times \frac{\partial O}{\partial In_o} \times \frac{\partial In_o}{\partial h_2} \times \frac{\partial h_2}{\partial w_{22}} \tag{6e}$$

$$\cdots \cdots$$

Updating the parameter,

$$w_i' = w_i - \eta \cdot \delta_i \tag{7}$$

η is learning rate.

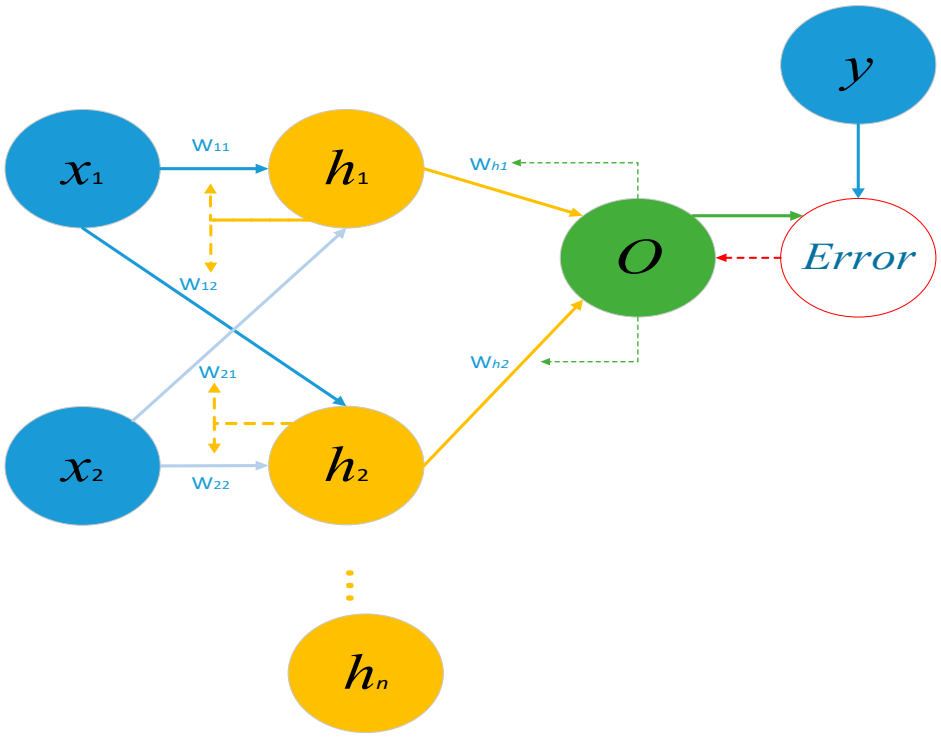

Figure 6. The typical data flow between nodes of BP algorithm with single hidden layer.

4.3. Learning Rate and Genetic Algorithm (GA)

The value of η is quite important to the truth-weight during the upper functional calculation: if the rate is too small then it affects the rate of convergence; η too high might ignore the extreme points and cause the algorithm to oscillate. It is the key element in the BP algorithm to determine the convergence rate and the accuracy of the weight value.

Due the importance of the study value, then we still have few ways to work it out approximately, but not exactly. Some research suggests that $0 < \eta_1 < 1/2 < \eta_2 < 1$ would

be satisfied. Under such condition, the optimal learning rate will belong to the acceptable interval [16]. Some programming manuals just roughly set the η to 0.001 or 0.01, called experimental validation. Here, we introduce a new genetic algorithm (GA) method to solve the constrained and unconstrained problems for optimization based on a natural selection process that simulates the biological evolution. In short, GA calculation is a more precise interval of the learning rate than other ways.

The proposed GA proceeds as the following steps. First, generate a BP parameter vector x (which contains η learning rate) with standard initial values which are common in literates ($0 < \eta < 1$). Then, create a mutated edition of x called y within the evolutionary circuit through Gaussian mutation while keeping the same σ for all elements. Afterwards, train Ax with BP parameters specified in x for a total of ρ era and repeat the same for Ay with y. Corresponding convergence errors are obtained after the networks are both trained, which are called $E(x)$ and $E(y)$, respectively. These error values will be used to examine which ANN and parameter vector will survive for subsequent generation [17]. The GA processing would be terminated as the $E(y)$ below the goal error or number of generations is reached and the best corresponding learning rate was obtained. We make this GA program run several times under the same conditions, so a series of learning rates are available. Now, the new interval should be updated based on those GA running results by one statistical prediction method. This kind of estimation method is called maximum likelihood estimation (MLE).

4.4. Maximum Likelihood Estimation (MLE)

Maximum likelihood estimation (MLE) is a technology to estimate parameters for a given distribution through the observed data. For example, if the known population follows a normal distribution but the mean and variance are not certain, MLE can be used to estimate the two parameters within the limited sample of the population by means of finding the particular values of the mean and variance, then the most likely results can be observed. The target of MLE is to identify the population that most probably generates the sample [18,19]. In this paper, those learning rates present a number of statistical standpoints, and the data vector $\eta = (\eta_1, \eta_2, \cdots, \eta_n)$ is the sample from an unknown population.

5. Experiments and Results

Figure 1 shows the experimental diagram, which exhibits the correlation between the different laser density, temperature, and the calculated efficiency during the PV process of the WPT. In this paper, we obtained 280 datasets under the series of laser density shown in Table 1.

Table 1. Laser density in LC experiments.

Laser Density (KW/m^2)	0.1	2	3	4.52	6
Sample Numbers	45	77	20	104	34

We used the BP algorithm in Matlab to generate the forecasted data without considering parameter optimization and especially taking the learning rate at 0.01 and 0.1; the results are shown in Figures 7 and 8. Here, an unexpected discovery was found, that the 0.1 value is more accurate than the 0.01 value. It was speculated that the value 0.01 is too small in gradient descent, thus the algorithm calculation limit was met before it reached the best value. That is the reason for the opposite BP result in our opinion.

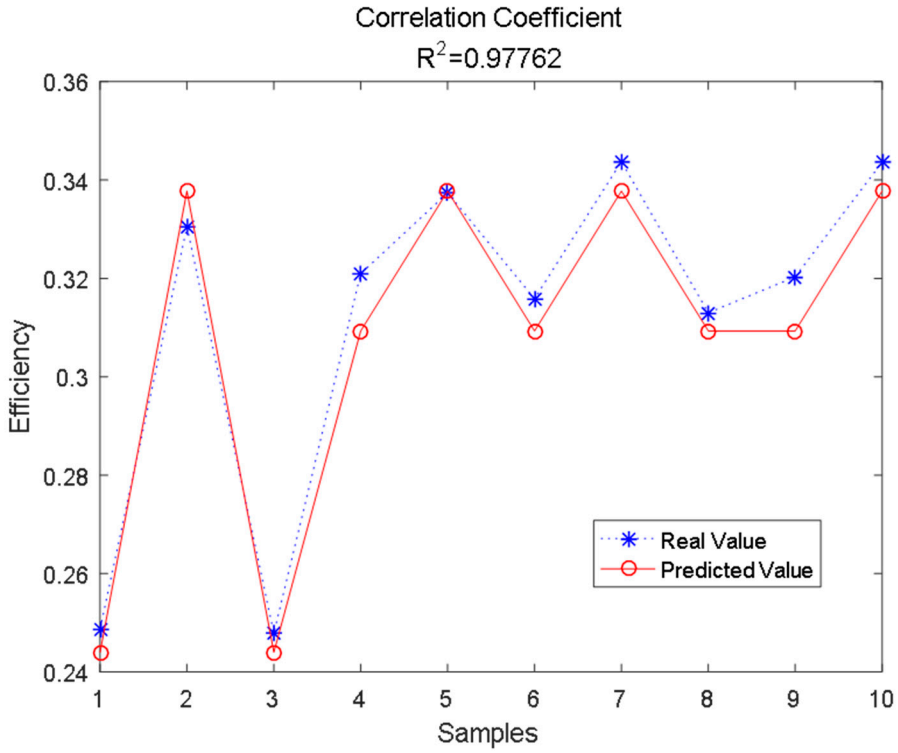

Figure 7. Efficiency predicted value by BP without learning rate optimization (η = 0.1).

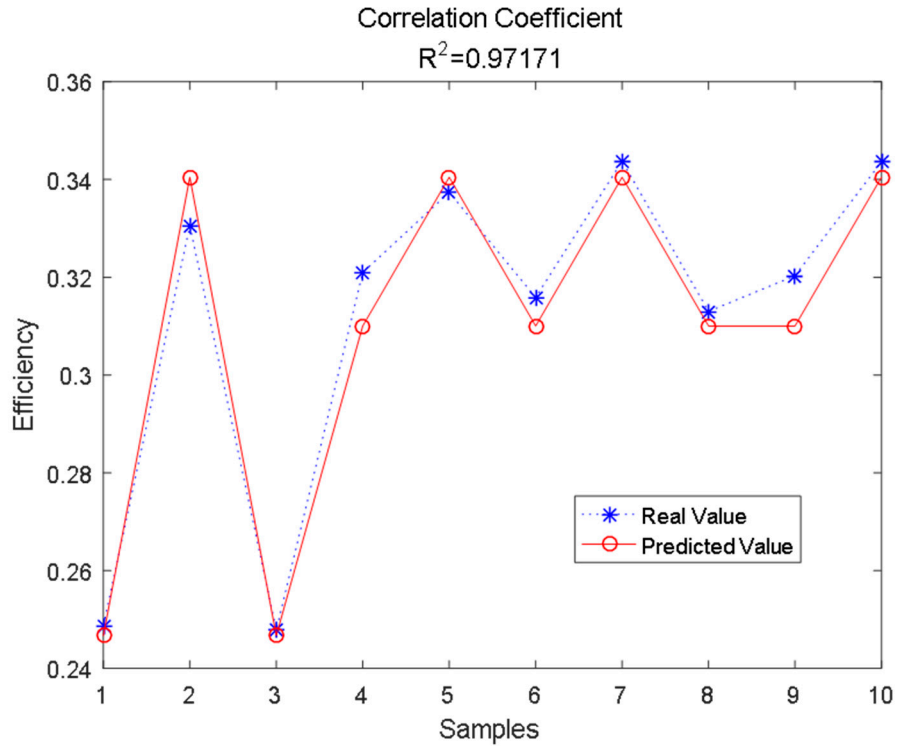

Figure 8. Efficiency predicted value by BP without learning rate optimization (η = 0.01).

The next step is optimizing the learning rate by GA, and the corresponding elements were set as shown in Table 2.

Table 2. GA parameter settings.

Learning Rate Interval	Population	Crossing-over	Mutation	Generation
0.00~1.00	50	0.8	0.1	10

The GA optimization results are shown in Figure 9, and a new interval could be drawn from the diagram, approximately between 0.4 and 0.6, compared with the old interval. The new learning rates were applied into the algorithm while the new result was updated as below in Figures 10 and 11.

Figure 9. 10 Best learning rate value after GA optimization.

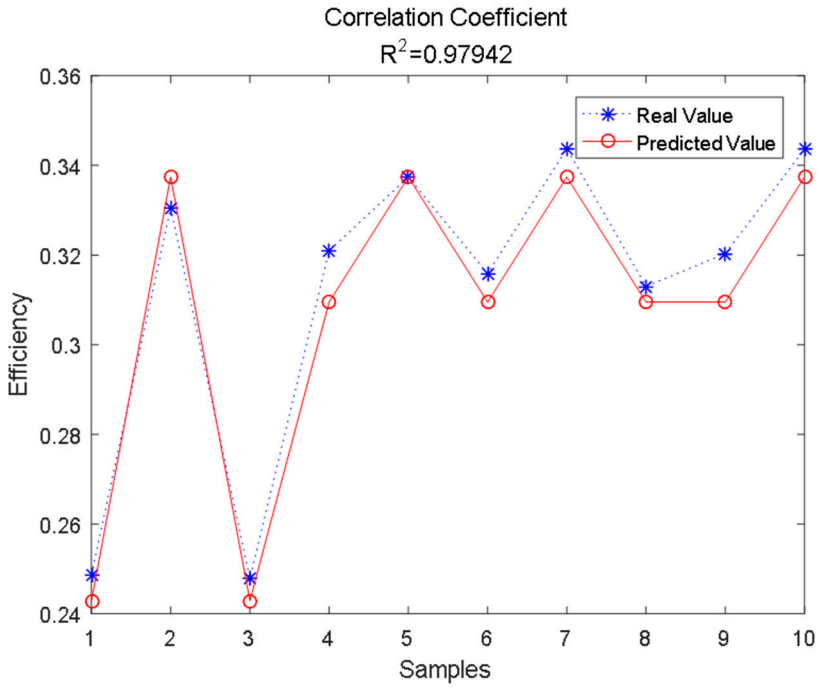

Figure 10. Efficiency predicted value by BP with learning rate optimization (η = 0.3924).

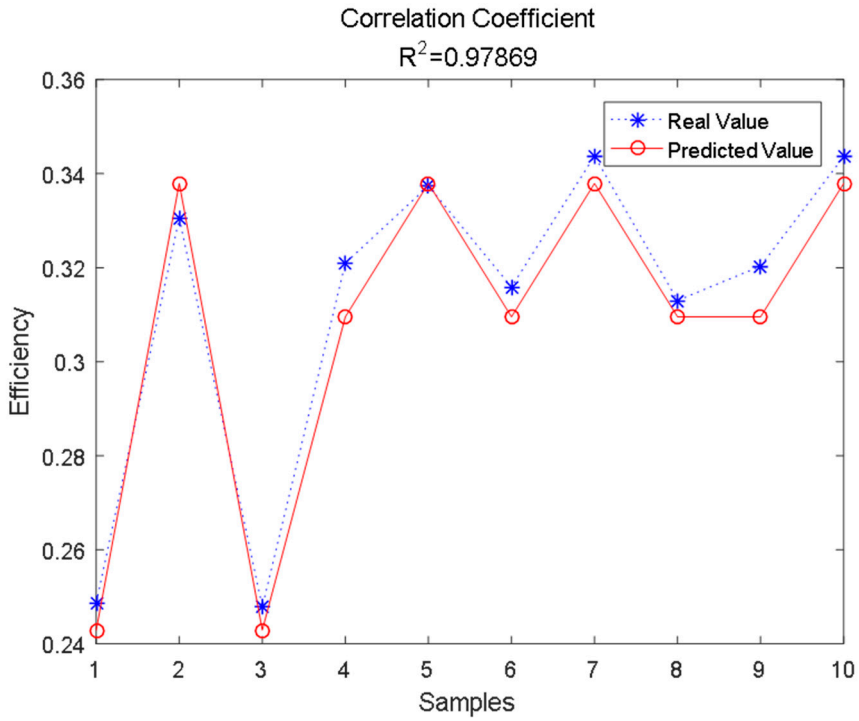

Figure 11. Efficiency predicted value by BP with learning rate optimization (η = 0.4934).

Comparing the above four results, we can make it clear that optimizing the learning rate increases good results of the data. While considering the measuring error and the random error, we introduce some random choice between BP datasets. After several times running the test, we obtained the best predicted value at minimum error. The BP algorithm with learning rate optimization results is showed in Figures 12 and 13.

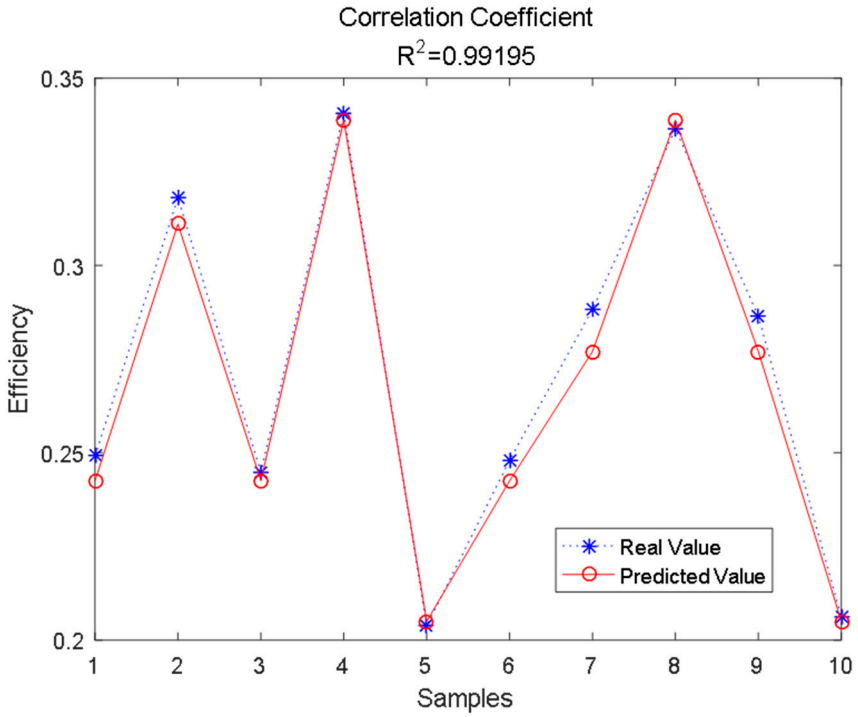

Figure 12. Efficiency predicted value by BP with learning rate optimization (η = 0.01).

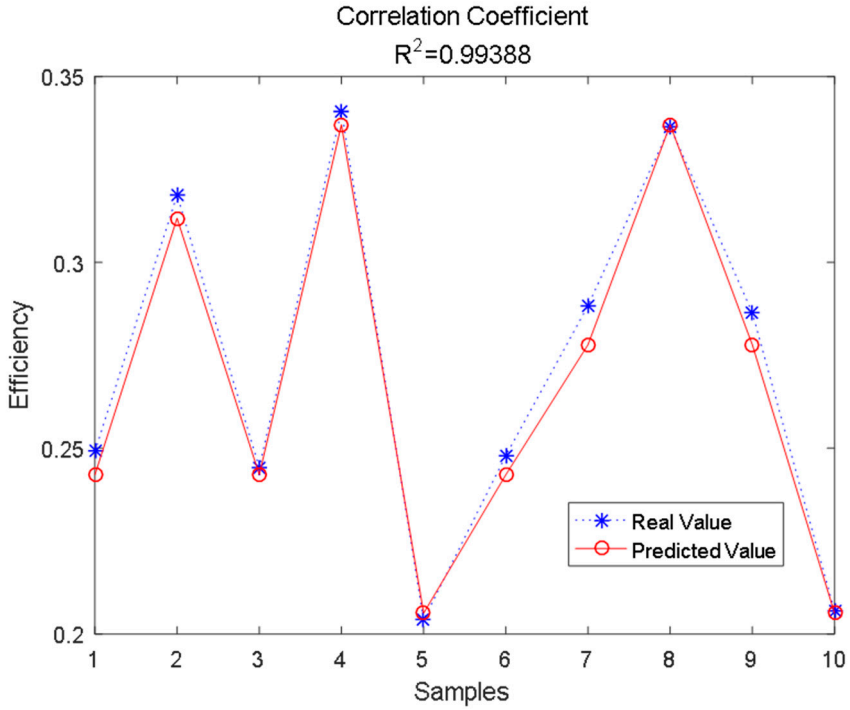

Figure 13. Efficiency predicted value by BP with learning rate optimization (η = 04934).

6. Discussion and Conclusions

This paper provided an accurate prediction method of the LC efficiency based on laser intensity and the temperature in the WPT system, which relied on ANN framework simulating human brain function. Laser intensity and the temperature were set as two input nodes, and LC efficiency as the output. The parameters were connected through hidden nodes and weights, and BP algorithm was used to modify the weights of the ANN. Then, after the whole network was trained well, the results were also better modulated. In order to optimize the key parameters in BP, this paper selected the learning rate as a sample for GA to memorize. Slightly superior results were achieved with GA application. Overall, our method obtained believable results through the experiment datasets. The maximum correlation coefficient reached 0.99388. Extensive experiments carried out show that this method improves the LC application and provides a fresh method for energy supply of WPT to IoT devices.

Author Contributions: Conceptualization, C.W.; methodology, H.T.; software, C.W.; validation, I.A.; investigation, G.L.; resources, H.Z.; data curation, C.W.; writing—original draft preparation, C.W.; writing—review and editing, G.L.; visualization, G.L.; supervision, J.L.; project administration, J.L.; funding acquisition, J.L. All authors have read and agreed to the published version of the manuscript.

Funding: We sincerely acknowledge the financial support from the National Defense Basic Scientific Research Program of China (No. JCKY2016606C002), the Shanghai Aerospace Science and Technology Innovation Fund (No. SAST20161113), and the National Natural Science Foundation of China (No. 11774176).

Institutional Review Board Statement: Not applicable.

Informed Consent Statement: Not applicable.

Data Availability Statement: Not applicable.

Conflicts of Interest: The authors declare no conflict of interest.

References

1. Sun, K.; Fan, R.; Zhang, X.; Zhang, Z.; Shi, Z.; Wang, N.; Xie, P.; Wang, Z.; Fan, G.; Liu, H.; et al. An overview of metamaterials and their achievements in wireless power transfer. *J. Mater. Chem. C* **2018**, *6*, 2925–2943. [CrossRef]
2. Wang, C.; Li, G.; Zhang, H.; Lu, J. The enhancement of the InGaAs solar cells by the thermoelectric generation technology under the continuous laser exposure. In Proceedings of the 5th International Symposium on Laser Interaction with Matter, LIMIS 2018, Changsha, China, 11–13 November 2018; pp. 110460C-1–110460C-9.
3. Ejaz, W.; Naeem, M.; Shahid, A.; Anpalagan, A.; Jo, M. Efficient Energy Management for the Internet of Things in Smart Cities. *IEEE Commun. Mag.* **2017**, *55*, 84–91. [CrossRef]
4. Nguyen, A.; Santos, P.M.; Rosa, M.; Aguiar, A. Study on Solar-powered IoT Node Autonomy. In Proceedings of the 2018 IEEE International Smart Cities Conference (ISC2), Kansas City, MO, USA, 16–19 September 2018; pp. 1–2.
5. Mukherjee, J.; Jarvis, S.; Perren, M.; Sweeney, S.J. Efficiency limits of laser power converters for optical power transfer applications. *J. Phys. D-Appl. Phys.* **2013**, *46*, 264006. [CrossRef]
6. Yugami, H.; Kanamori, Y.; Arashi, H.; Niino, M.; Moro, A.; Eguchi, K.; Okada, Y.; Endo, A. Field experiment of laser energy transmission and laser to electric conversion. In Proceedings of the 1997 32nd Intersociety Energy Conversion Engineering Conference, Honolulu, HI, USA, 27 July–1 August 1997; Part 1, pp. 625–630.
7. After the Challenge: Laser Motive. Available online: https://www.nasa.gov/directorates/spacetech/centennial_challenges/after_challenge/lasermotive.html (accessed on 15 March 2022).
8. Green, M.A.; Dunlop, E.D.; Hohl-Ebinger, J.; Yoshita, M.; Kopidakis, N.; Hao, X. Solar cell efficiency tables (version 58). *Prog. Photovolt. Res. Appl.* **2021**, *29*, 657–667. [CrossRef]
9. Green, M.A.; Dunlop, E.D.; Hohl-Ebinger, J.; Yoshita, M.; Kopidakis, N.; Hao, X. Solar cell efficiency tables (version 59). *Prog. Photovolt. Res. Appl.* **2022**, *30*, 3–12. [CrossRef]
10. Nelson, J. *The Physics of Solar Cells*; Imperial College Press: London, UK, 2003.
11. Power-Sources, Shanghai Institute of Space Power-Sources. *Physics Power Technology*; Science Press: Beijing, China, 2015.
12. Kalyuzhnyy, N.A.; Emelyanov, V.M.; Evstropov, V.V.; Mintairov, S.A.; Mintairov, M.A.; Nahimovich, M.V.; Salii, R.A.; Shvarts, M.Z. Optimization of photoelectric parameters of InGaAs metamorphic laser (lambda=1064 nm) power converters with over 50% efficiency. *Sol. Energy Mater. Sol. Cells* **2020**, *217*, 110710. [CrossRef]
13. Wang, C.; Li, G.; Ali, I.; Zhang, H.; Tian, H.; Lu, J. The Management of Energy Transformation through Laser Charging in WPT for 5G Application: Prediction Model of the In0.3Ga0.7As Solar Cell. *Wirel. Commun. Mob. Comput.* **2022**, *2022*, 5991154. [CrossRef]
14. Das, U.K.; Tey, K.S.; Seyedmahmoudian, M.; Mekhilef, S.; Idris, M.Y.I.; Van Deventer, W.; Horan, B.; Stojcevski, A. Forecasting of photovoltaic power generation and model optimization: A review. *Renew. Sustain. Energy Rev.* **2018**, *81*, 912–928. [CrossRef]
15. Basheer, I.A.; Hajmeer, M. Artificial neural networks: Fundamentals, computing, design, and application. *J. Microbiol. Methods* **2000**, *43*, 3–31. [CrossRef]
16. Yu, X.H.; Chen, G.A.; Cheng, S.X. Dynamic learning rate optimization of the backpropagation algorithm. *IEEE Trans. Neural Netw.* **1995**, *6*, 669–677. [CrossRef] [PubMed]
17. Parra, J.; Trujillo, L.; Melin, P. Hybrid back-propagation training with evolutionary strategies. *Soft Comput.* **2014**, *18*, 1603–1614. [CrossRef]
18. Contributed, Brilliant.org. Maximum Likelihood Estimation (MLE). Available online: https://brilliant.org/ (accessed on 25 March 2022).
19. Myung, I.J. Tutorial on maximum likelihood estimation. *J. Math. Psychol.* **2003**, *47*, 90–100. [CrossRef]